ACS Combinatorial Science

Research Article

Cite This: ACS Comb. Sci. 2019, 21, 198−206

pubs.acs.org/acscombsci

Bicyclic RGD Peptides with Exquisite Selectivity for the Integrin $\alpha_v\beta_3$ Receptor Using a "Random Design" Approach

Dominik Bernhagen,[†] Vanessa Jungbluth,[‡] Nestor Gisbert Quilis,[‡] Jakub Dostalek,[‡] Paul B. White,[§] Kees Jalink,[∥] and Peter Timmerman*[,†,⊥]

[†]Pepscan Therapeutics, Zuidersluisweg 2, 8243 RC Lelystad, The Netherlands

[‡]Biosensor Technologies, AIT Austrian Institute of Technology GmbH, Konrad-Lorenz-Straße 24, 3430 Tulln, Austria

[§]Institute for Molecules and Materials, Radboud University, Heyendaalseweg 135, 6525 AJ Nijmegen, The Netherlands

[∥]The Netherlands Cancer Institute, Plesmanlaan 21, 1066 CX Amsterdam, The Netherlands

[⊥]Van't Hoff Institute for Molecular Sciences, University of Amsterdam, Science Park 904, 1098 XH Amsterdam, The Netherlands

Supporting Information

ABSTRACT: We describe the identification of bicyclic RGD peptides with high affinity and selectivity for integrin $\alpha_v\beta_3$ via high-throughput screening of partially randomized libraries. Peptide libraries (672 different compounds) comprising the universal integrin-binding sequence Arg-Gly-Asp (RGD) in the first loop and a randomized sequence XXX (X being one of 18 canonical L-amino acids) in the second loop, both enclosed by either an L- or D-Cys residue, were converted to bicyclic peptides via reaction with 1,3,5-tris(bromomethyl)benzene (**T3**). Screening of first-generation libraries yielded lead bicyclic inhibitors displaying submicromolar affinities for integrin $\alpha_v\beta_3$ (e.g., $\mathbf{C}_{T3}$HEQ$\mathbf{c}_{T3}$RGD$\mathbf{c}_{T3}$, IC_{50} = 195 nM). Next generation (second and third) libraries were obtained by partially varying the structure of the strongest lead inhibitors and screening for improved affinities and selectivities. In this way, we identified the highly selective bicyclic $\alpha_v\beta_3$-binders $\mathbf{C}_{T3}$HPQ$\mathbf{c}_{T3}$RGD$\mathbf{c}_{T3}$ (IC_{50} = 30 nM), $\mathbf{C}_{T3}$HPQ$\mathbf{C}_{T3}$RGD$\mathbf{c}_{T3}$ (IC_{50} = 31 nM), and $\mathbf{C}_{T3}$HSQ$\mathbf{C}_{T3}$RGD$\mathbf{c}_{T3}$ (IC_{50} = 42 nM) with affinities comparable to that of a knottin-RGD-type peptide (32 amino acids, IC_{50} = 38 nM) and outstanding selectivities over integrins $\alpha_v\beta_5$ (IC_{50} > 10000 nM) and $\alpha_5\beta_1$ (IC_{50} > 10000 nM). Affinity measurements using surface plasmon-enhanced fluorescence spectroscopy (SPFS) yielded K_d values of 0.4 and 0.6 nM for the Cy5-labeled bicycle $\mathbf{C}_{T3}$HPQ$\mathbf{c}_{T3}$RGD$\mathbf{c}_{T3}$ and RGD "knottin" peptide, respectively. In vitro staining of HT29 cells with Cy5-labeled bicycles using confocal microscopy revealed strong binding to integrins in their natural environment, which highlights the high potential of these peptides as markers of integrin expression.

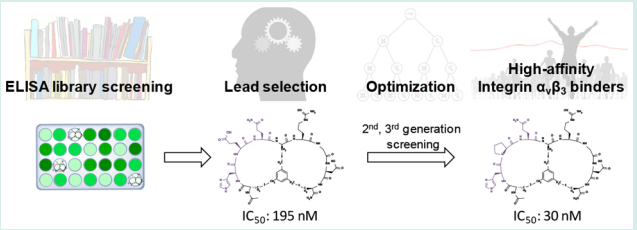

KEYWORDS: *RGD, integrin, peptide−protein interaction, ELISA, bicyclic peptide, library screening, SPFS*

INTRODUCTION

(Multi)cyclic peptides represent an important platform in drug development owing to their unique properties, such as conformational restriction and low toxicity. Peptides produced by nature, for example, romidepsin, vancomycin, and ciclosporin, and semisynthetic peptides such as dalbavancin are established peptide-based drugs.[1] Over the past years, the bicyclic CLIPS-peptide platform, first described by our group,[2] has attracted considerable interest by combining high target affinities and selectivities with appreciable proteolytic stabilities.[3] It has been actively explored to provide a variety of (enzyme) inhibitors. For example, Heinis et al. used the technology in combination with phage-display library screening to identify a bicyclic peptide inhibitor ($\mathbf{AC}_{T3}$SDRFRN$\mathbf{C}_{T3}$PADEAL$\mathbf{C}_{T3}$G, **T3** = 1,3,5-trimesitylenyl scaffold), displaying nanomolar affinity to plasma kallikrein (K_i = 1.5 nM).[4] Here, the consensus motif SDRFRN was identified in the first round of selection, followed by sequential optimization of the second loop. Notably, the activities of the linear peptides were at least 250-fold lower in comparison to the corresponding **T3**-bicycles. The same group also reported a bicyclic peptide inhibitor ($\mathbf{AC}_{T3}$SRYEVD$\mathbf{C}_{T3}$RGRGSA$\mathbf{C}_{T3}$G) of urokinase-type plasminogen activator (uPA) with a K_i of 53 nM[5] and, most recently, an active bicyclic inhibitor ($\mathbf{AC}_{T3}$HSR$\mathbf{C}_{T3}$PQLPP$\mathbf{C}_{T3}$G) of sortase A (K_i = 1.1 μM).[6] Luzi et al. also explored the high-throughput potential of CLIPS phage-display libraries to identify a potent bicyclic inhibitor ($\mathbf{AC}_{T3}$PP$\mathbf{C}_{T3}$LWQVL$\mathbf{C}_{T3}$, K_d = 10 nM) to TNFα, one of the key mediators of several inflammatory disorders.[7] As an alternative to this, Lian et al. developed a one-bead two-compound screening technology to identify double-digit nanomolar bicyclic peptide inhibitors for protein tyrosine phosphatase 1B (PTP1B), a type II diabetes target,[8] with the target-binding sequence in the first loop and

Received: September 20, 2018
Revised: December 4, 2018
Published: January 9, 2019

the cell-penetrating peptide FΦRRRQ (Φ: L-naphthylalanine) in the second loop. Recently, the same group reported a submicromolar bicyclic inhibitor for K-Ras, combining a cell-permeable peptide sequence in the first loop with the K-Ras binding motif AJFRnΨID (J, D-Leu; Ψ, L-propargylglycine) in the second loop.[9]

In this paper we describe a novel approach to identify potent bicyclic binders to integrin $\alpha_v\beta_3$ by combining rational design[10] with medium diversity (total of 672 peptides). These bicycles combine a "fixed" RGD loop ("Design") with a second loop (XXX, "Random") that further supports the RGD-integrin affinity and also brings selectivity into the peptide. Integrins represent a family of cell adhesion receptors[11] that are potential targets for novel therapeutic agents resulting from their significant role in pathological processes. A major contribution to the investigation of integrin-binding peptides was made by Kessler and co-workers, who developed the potent $\alpha_v\beta_3$ antagonist cilengitide,[12] and other cyclopeptides with decent affinities for integrins, such as $\alpha_v\beta_3$, $\alpha_5\beta_1$, and $\alpha_6\beta_1$.[13a−g] In addition, integrin affinity tuning via conformational confinement on of the RGD peptide on surfaces has been reported.[13h−j] Recently, Cochran and co-workers described a family of high-affinity integrin-binding "cystine-knot" (knottin) RGD peptides, which are considered great candidates for drug development.[14] However, these disulfide-rich peptides basically do not express any selectivity in binding to the integrins $\alpha_v\beta_3$, $\alpha_5\beta_1$, and $\alpha_v\beta_5$. Here we describe a set of bicyclic RGD peptides that display both high affinities and outstanding selectivities for $\alpha_v\beta_3$. Moreover, we also developed a similar set of binders with selectivities for the integrin $\alpha_5\beta_1$, the results of which will be disclosed elsewhere. We consider this combined "random-design" approach also highly suited for identifying high-affinity and -selectivity binders to different ECM target proteins based on e.g. the laminin-binding YIGSR- or IKVAV-peptide motifs.

RESULTS AND DISCUSSION

General Procedure for Library Screening. Our approach involves the design of partially randomized libraries of small, RGD-containing bicyclic CLIPS (chemical linkage of peptides onto scaffolds)[15] peptides to be used in an iterative affinity and selectivity optimization process for the integrin receptor $\alpha_v\beta_3$. We used libraries of "label-free" peptides comprising acetylated N-termini and C-terminal amides, the individual $\alpha_v\beta_3$-binding activities of which were evaluated by measuring the extent of inhibition of biotinylated knottin-RGD binding to integrin $\alpha_v\beta_3$ using a recently published competition ELISA setup (see Table S-1 in the Supporting Information).[16] A schematic representation of this setup is given in the Supporting Information of ref 16. At first, all 672 bicyclic RGD peptides were screened for inhibition at the highest concentration (1 mM). For the top 96 hits from the first screening (top 30 for second and third generations), which showed at least 90% inhibition at 1 mM, a second screening was performed at lower concentration (2.5−10 μM) to determine their affinities more accurately. Finally, the best binders were resynthesized and HPLC-purified, followed by determination of the IC_{50} values.

Design and Synthesis of RGD Peptide Libraries. We designed linear peptide libraries consisting of two separate binding motifs surrounded by three cysteines. The first motif contains the well-known RGD sequence that should provide the basal integrin affinity, while the second motif contains a randomized sequence "XXX", which is intended to support binding of the RGD loop and also to provide integrin selectivity. The motifs are enclosed by cysteines, which ensure the double CLIPS cyclization (**T3**, Figure 1) and hence the formation of a bicyclic peptide comprising two different loops.

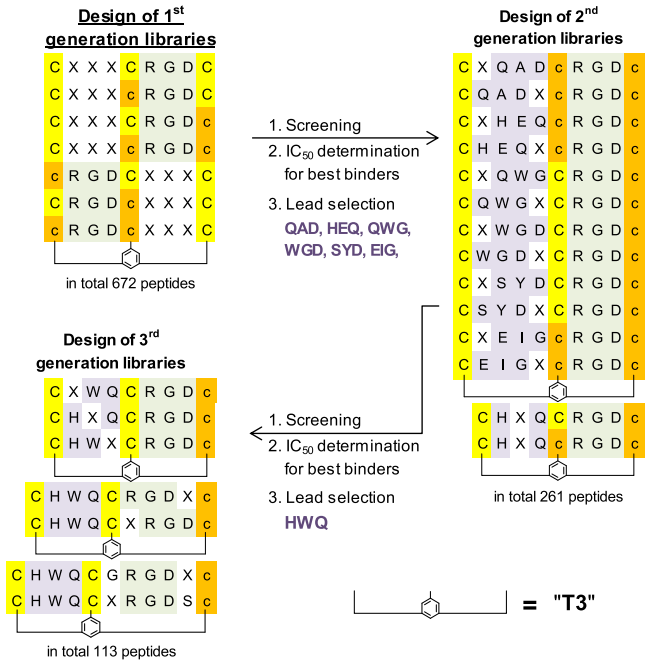

Figure 1. Methodology for the design of high-affinity bicyclic peptides to integrin $\alpha_v\beta_3$. X represents any canonical L-amino acid. L-cysteines are indicated in yellow, D-cysteines in orange, and RGD motifs in green. Lead motifs are shown in purple.

The primary challenge was to determine the proper size of both the RGD and the random X(X)$_n$X loop. The well-known integrin binder cilengitide (*cyclo*-[V(*N*-Me)RGDf])[12] consists of five amino acids. In a bicyclic peptide, a similar 5-mer loop is generated by enclosing the 3-mer RGD sequence with two cysteines; hence, the minimal integrin-binding motif CRGDC was selected. We kept the RGD loop size constant in the first-generation library and checked for further optimization at a later stage. For the second, randomized loop, we considered a trimer XXX motif suitable to provide the required level of structural and conformational diversity. When all natural amino acids (except cysteine and methionine) are included, there are 324 (18^2) possible variants of the dimer motif XX, 5832 possible trimer sequences XXX, and 104976 variants for the tetramer motif XXXX. Therefore, 96 different XXX motifs would cover 1.8% of the total viable natural L-tripeptide space, which is reasonable when one considers the chance to overlook a high-affinity integrin binder after several rounds of optimization, in particular in comparison to the 0.09% coverage of structural space when a tetrameric XXXX motif is used.

The RGD motif was located either in the C-terminal/right loop and the XXX sequence in the N-terminal/left loop or vice versa. A total of 96 random XXX sequences were generated for each loop by using the software program R. In view of the apparent effect of D-amino acids on integrin binding affinity,[12,17] additional sublibraries comprising different combinations of L- and D-cysteines were also designed. Hence, the entire first-generation library consisted of four sublibraries with

DOI: 10.1021/acscombsci.8b00144
ACS Comb. Sci. 2019, 21, 198−206

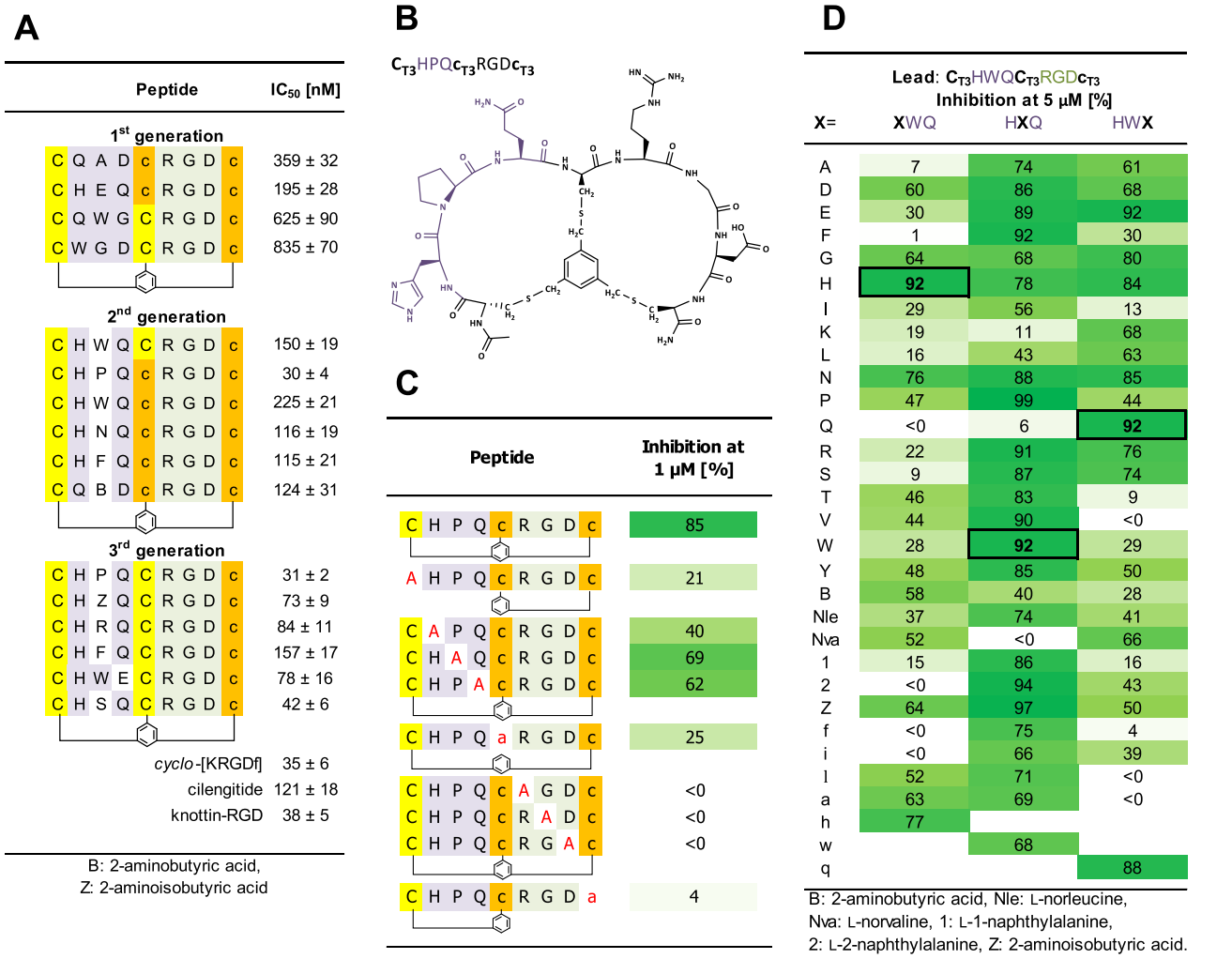

Figure 2. (A) IC_{50} values for first-, second-, and third-generation bicyclic integrin $\alpha_v\beta_3$ binders. Each concentration was tested in triplicate. IC_{50} values were calculated via nonlinear regression analysis. Inhibition values were calculated on the basis of absorbance when the bicyclic competitor was not present (0%, $OD_{405} \approx 1.8$), or when nonbiotinylated knottin-RGD was added at 30 μM (100%, $OD_{405} \approx 0.2$). (B) Molecular structure of the second-generation bicycle withthe highest integrin $\alpha_v\beta_3$ affinity. (C) Alanine replacement analysis for the bicycle $\mathbf{C}_{T3}$HPQ$\mathbf{c}_{T3}$RGD$\mathbf{c}_{T3}$. (D) Full amino acid replacement analysis (HWQ motif) of the bicycle $\mathbf{C}_{T3}$HWQ$\mathbf{C}_{T3}$RGD$\mathbf{c}_{T3}$ using nonpurified peptides. If absorbances were not lower but higher in the presence of nonlabeled peptide, inhibition values were reported as <0. Boldface, framed values refer to the lead peptide. D-Amino acids are represented as small letters.

96 random sequences in the left loop and three sublibraries with random sequences in the right loop, giving a total number of 672 different **T3** bicycles ($\mathbf{C}_{T3}$XXX$\mathbf{C}_{T3}$RGD$\mathbf{C}_{T3}$/ $\mathbf{C}_{T3}$XXX$\mathbf{c}_{T3}$RGD$\mathbf{C}_{T3}$/ $\mathbf{C}_{T3}$XXX$\mathbf{C}_{T3}$RGD$\mathbf{c}_{T3}$/ $\mathbf{C}_{T3}$XXX$\mathbf{c}_{T3}$RGD$\mathbf{c}_{T3}$/ $\mathbf{c}_{T3}$RGD$\mathbf{C}_{T3}$XXX$\mathbf{C}_{T3}$/ $\mathbf{C}_{T3}$RGD$\mathbf{c}_{T3}$XXX$\mathbf{C}_{T3}$/$\mathbf{c}_{T3}$RGD$\mathbf{c}_{T3}$XXX$\mathbf{C}_{T3}$, Figure 1). After these libraries were screened for binding to integrin $\alpha_v\beta_3$ (method described below), various lead motifs for next-generation libraries were derived from the sequences of the best binders. The second loop in the second-generation libraries comprised (i) all first-generation lead sequences (e.g., QAD), extended by one amino acid (XQAD or QADX), and (ii) a full replacement set of the second amino acid (X in the HXQ motif, in view of multiple positive hits: HEQ/2xHLQ). After the best second-generation $\alpha_v\beta_3$-binders were identified, a set of third-generation libraries was designed on the basis of (i) a full set of replacement variants (86 peptides) based on the HWQ motif and (ii) extension of the RGD loops on either or both ends with one amino acid (e.g., RGDX/XRGD or GRGDX/XRGDS) while the second loop HWQ was kept constant.

Screening Bicyclic Peptide Libraries for $\alpha_v\beta_3$-Bindin. About 4% of the 672 first-generation bicyclic RGD peptides showed OD_{405} values below 0.4, corresponding to more than 80% inhibition of knottin-RGD binding to $\alpha_v\beta_3$ (OD_{405} = 0.2, 100% inhibition; OD_{405} = 1.2, 0% inhibition). For the strongest $\alpha_v\beta_3$-binding bicycles, we observed an overrepresentation of peptides comprising the RGD motif in the C-terminal/right loop. Moreover, the best binders all had at least one D-Cys attached to the RGD sequence, either C-terminal or both N- and C-terminal, which is consistent with the results of Kessler et al., who reported enhanced integrin binding for (mono)cyclic peptides with a D-amino acid next to the RGD motif.[17] Furthermore, we also found that peptides comprising the motif HXQ (X = any L-amino acid) in the left loop mostly showed significant inhibition. Surprisingly, approximately 50% of the bicyclic RGD peptides showed OD_{405} values of higher than 2.0, even though the OD_{405} of pure biotinylated knottin-RGD peptide was only ~1.2. Apparently, those bicycles

DOI: 10.1021/acscombsci.8b00144
ACS Comb. Sci. 2019, 21, 198−206

somehow activate either the $\alpha_v\beta_3$ for knottin-RGD binding or vice versa. Another possibility might be that these bicycles promiscuously bind to the integrin and streptavidin. In any event, at this point we did not further investigate those bicycles or considered them of interest as potent and selective $\alpha_v\beta_3$ binders.

We then retested the best 96 hits from the first screening using only a 100-fold excess (10 μM) over the knottin-RGD peptide, and from these only 28% (27 peptides) showed >50% inhibition. The four strongest binders from both screenings ($\mathbf{C}_{T3}$QAD$\mathbf{c}_{T3}$RGD$\mathbf{c}_{T3}$, $\mathbf{C}_{T3}$HEQ$\mathbf{c}_{T3}$RGD$\mathbf{c}_{T3}$, $\mathbf{C}_{T3}$QWG$\mathbf{C}_{T3}$RGD$\mathbf{c}_{T3}$, and $\mathbf{C}_{T3}$WGD$\mathbf{C}_{T3}$RGD$\mathbf{c}_{T3}$) were then resynthesized on a larger scale (20 μmol) and purified and their activities determined (195 nM < IC_{50} < 835 nM, Figure 2A). These values are still significantly higher than those determined for the knottin-RGD peptide itself (38 nM) and the *cyclo*-[KRGDf] peptide (35 nM). To further improve affinities, second-generation libraries were designed using the six best binders from first screenings as a lead, having (i) extended (4-mer) second loops, e.g. XQAD or QADX (total of 216 peptides, see Figure 1), (ii) a full set of replacements for the glutamate (E) of the motif HEQ (25 peptides), (iii) a set of 12 non-natural variants of various potent lead sequences (see the Supporting Information), and (iv) the best 8 hits from first-generation screenings. From the total set of 261 RGD bicycles 31% (82 peptides) showed >50% inhibition at 5 μM, while only 7% (18) showed even >70% inhibition. To further narrow down the selection, we performed a rescreening of the best 30 hits at 2.5 μM, in which only 6% of the peptides (15) showed >50% inhibition and only 2% (6 peptides) showed >70% inhibition. None of the six best binders comprised an extended 4-mer sequence (such as XQAD or WGDX), indicating the choice for a trimer sequence in the left loop was correct. Instead, five peptides comprised the HXQ motif (with X = W(2x)/P/N/F) and one the non-natural sequence Q[Abu]D (Abu = L-2-aminobutyric acid), with IC_{50} values (measured with HPLC-purified peptides) ranging from 30 nM ($\mathbf{C}_{T3}$HPQ$\mathbf{c}_{T3}$RGD$\mathbf{c}_{T3}$) to 225 nM ($\mathbf{C}_{T3}$HWQ$\mathbf{c}_{T3}$RGD$\mathbf{c}_{T3}$, Figure 2A). Molecular structures of the best $\alpha_v\beta_3$ inhibitors are shown in Figure 2B. Five of the six second-generation binders showed lower IC_{50} values in comparison to the best first-generation binder ($\mathbf{C}_{T3}$HEQ$\mathbf{c}_{T3}$RGD$\mathbf{c}_{T3}$, IC_{50} = 195 nM). The strongest binder, $\mathbf{C}_{T3}$HPQ$\mathbf{c}_{T3}$RGD$\mathbf{c}_{T3}$, displayed an IC_{50} value of 30 nM, which is comparable to that of knottin-RGD (38 nM) as reported by Kimura et al.[14a]

We then designed third-generation libraries comprising (i) a complete set of single-replacement variants for the second-generation lead HWQ (86 peptides) and (ii) 4-mer and 5-mer RGD loops extended by an additional amino acid (X) at either one or both ends, while the HWQ loop was kept constant (57 tetramer and 56 pentamer peptides, in total 113 peptides; Figure 1). From the total of ~200 bicycles that were screened at 5 μM, 35% (79 peptides) showed >50% inhibition, 18% (35 peptides) showed >70% inhibition, and only 4% (8 peptides) displayed >90% inhibition. In the rescreening of the best 20 hits (at 2.5 μM), 95% (19) of the peptides showed >80% inhibition, while only four peptides (20%) showed even >90% inhibition. The best six binders (i.e., $\mathbf{C}_{T3}$HPQ$\mathbf{C}_{T3}$RGD$\mathbf{c}_{T3}$, $\mathbf{C}_{T3}$H[Aib]Q$\mathbf{C}_{T3}$RGD$\mathbf{c}_{T3}$ (with Aib = 2-aminoisobutyric acid), $\mathbf{C}_{T3}$HRQ$\mathbf{C}_{T3}$RGD$\mathbf{c}_{T3}$, $\mathbf{C}_{T3}$HFQ$\mathbf{C}_{T3}$RGD$\mathbf{c}_{T3}$, $\mathbf{C}_{T3}$HWE$\mathbf{C}_{T3}$RGD$\mathbf{c}_{T3}$, and $\mathbf{C}_{T3}$HSQ$\mathbf{C}_{T3}$RGD$\mathbf{c}_{T3}$) were resynthesized and purified for activity testing in a concentration-dependent manner. The most active binder ($\mathbf{C}_{T3}$HPQ$\mathbf{C}_{T3}$RGD$\mathbf{c}_{T3}$, IC_{50} = 31 nM) differed only from the best second-generation binder, i.e. $\mathbf{C}_{T3}$HPQ$\mathbf{c}_{T3}$RGD$\mathbf{c}_{T3}$ (Figure 2A), in the configuration of the second cysteine. The other third-generation binders showed IC_{50} values ranging from 42 to 157 nM.

An alanine replacement study, in which each amino acid of the best $\alpha_v\beta_3$ binder $\mathbf{C}_{T3}$HPQ$\mathbf{c}_{T3}$RGD$\mathbf{c}_{T3}$ (85% inhibition at 1 μM) was sequentially replaced by L- or D-alanine, revealed significantly decreased affinities when R/G/D (<0%), H/P/Q (40−69%), or either one of the L-/D-cysteine residues formed monocyclic peptides (4−25%, Figure 2C). Furthermore, a full replacement study on the HWQ loop of the second-generation binder $\mathbf{C}_{T3}$HWQ$\mathbf{c}_{T3}$RGD$\mathbf{c}_{T3}$ (Figure 2D) clearly revealed the much higher importance of H (histidine) and Q (glutamine) in comparison to W (tryptophan). This obviously is the reason why so many W variants showed up as potentially improved binders.

Essence of Cysteine Residues. We also tested variants of the second-generation lead $\mathbf{C}_{T3}$HWQ$\mathbf{C}_{T3}$RGD$\mathbf{c}_{T3}$ (27 peptides in total) in which one, two, or all three cysteines were replaced by the non-natural variants L-/D-homocysteine (hC/hc), or L-/D-penicillamine (Pen/pen) (Figure S2 in the Supporting Information). All mutations showed a clear decrease in $\alpha_v\beta_3$ binding, but the decrease was much stronger for the Pen variants in comparison to the hC variants. For example, $\mathbf{C}_{T3}$HWQ$(\mathbf{hC})_{T3}$RGD$\mathbf{c}_{T3}$ and $\mathbf{C}_{T3}$HWQ$\mathbf{C}_{T3}$RGD$(\mathbf{hc})_{T3}$ showed 85/53% and 80/37% inhibition at 10 or 1 μM (88/55% for the lead), whereas the corresponding Pen variants $\mathbf{C}_{T3}$HWQ$(\mathbf{Pen})_{T3}$RGD$\mathbf{c}_{T3}$ and $\mathbf{C}_{T3}$HWQ$\mathbf{C}_{T3}$RGD$(\mathbf{pen})_{T3}$ basically showed no measurable inhibition (i.e., 0%) at 10 μM. Occasionally the Pen variants did show activities comparable to those of the corresponding hC variants, as for $(\mathbf{Pen})_{T3}$HWQ$\mathbf{C}_{T3}$RGD$\mathbf{c}_{T3}$ (31%/8% at 10/1 μM) and $(\mathbf{hC})_{T3}$HWQ$\mathbf{C}_{T3}$RGD$(\mathbf{hc})_{T3}$ (20%/12% at 10/1 μM), but an improved affinity was never observed, suggesting that the additional methyl groups in penicillamine largely abolish the integrin−bicycle interaction.

Single-Loop Controls. To illustrate the essence of the bicyclic peptide format for binding activity, we synthesized and tested the single-loop variants of some of the first-generation binders in which one of the three D-/L-cysteines was replaced by alanines. The single-loop variants (C/A-1, A$\mathbf{QAD}\mathbf{c}_{mT2}RGD\mathbf{c}_{mT2}$; c/a-2, $\mathbf{C}_{mT2}$QADaRGD$\mathbf{c}_{mT2}$; c/a-3, $\mathbf{C}_{mT2}$QAD$\mathbf{c}_{mT2}$RGDa) were synthesized using 1,3-bis-(bromomethyl) benzene (**mT2**), which is the bivalent half of the trivalent **T3** scaffold (for more detailed information on peptides constrained via CLIPS scaffolds **T3** and **mT2**, see refs 2, 3b, 4, 5, and 10). For $\mathbf{C}_{T3}$QAD$\mathbf{c}_{T3}$RGD$\mathbf{c}_{T3}$, $\alpha_v\beta_3$ binding strongly decreased on opening the QAD loop (79% to 7% for C/A-1), the RGD loop (79% to 0% for c/a-3), or both (79% to 32% for c/a-2) (see Table S-2 in the Supporting Information). Likewise, a vast decrease in affinity was observed for single-loop variants of bicyclic peptides $\mathbf{C}_{T3}$HEQ$\mathbf{c}_{T3}$RGD$\mathbf{c}_{T3}$ (from 92% to 22% (C/A-1), 28% (c/a-3), and 22% (c/a-2)) and $\mathbf{C}_{T3}$WGD$\mathbf{C}_{T3}$RGD$\mathbf{c}_{T3}$ (from 75% to 52% (C/A-1), 8% (c/a-3), and 23% (C/A-2)), which exemplifies the essence of constraining both loops for optimal $\alpha_v\beta_3$ inhibition. Moreover, the corresponding single-loop RGD peptides also showed much lower binding values at 10 μM in comparison to the best bicyclic binders ($\mathbf{C}_{mT2}$RGD$\mathbf{C}_{mT2}$, 23%; $\mathbf{C}_{mT2}$RGD$\mathbf{c}_{mT2}$, 57%; $\mathbf{c}_{mT2}$RGD$\mathbf{c}_{mT2}$, 41% (Table S-2 in the Supporting Informtion), which underscores the importance of the second loop for integrin $\alpha_v\beta_3$ binding.

DOI: 10.1021/acscombsci.8b00144
ACS Comb. Sci. 2019, 21, 198−206

Binding of HPQ Bicycles to Streptavidin. The fact that we identified high-affinity $\alpha_v\beta_3$ binders comprising the HPQ motif via a competition ELISA may complicate the assay interpretation, as this motif is known to bind to streptavidin under certain conditions.[18] In order to exclude the possibility that bicycles containing HPQ or similar motifs directly interact with streptavidin, and so would falsely indicate a strong $\alpha_v\beta_3$ interaction, we directly measured the ability of a series of bicyclic and monocyclic peptides comprising the HPQ motif to bind to streptavidin-HRP in a simple binding ELISA (Table S-3 in the Supporting Information). As expected, none of the bi- and monocyclic peptides showed detectable binding to Strep-HRP in the 0.005−30 μM concentration range as used in the competition ELISA. Only the bicyclic peptide $\mathbf{C}_{T3}$HFQ$\mathbf{C}_{T3}$RGD$\mathbf{c}_{T3}$ (OD ≈ 0.2) and monocyclic control $\mathbf{C}_{mT2}$HPQ$\mathbf{c}_{mT2}$ showed very weak binding to Strep-HRP at 100 μM (OD ≈ 0.4), but this can by no means be held responsible for the fact that bicycles $\mathbf{C}_{T3}$HPQ$\mathbf{C}_{T3}$RGD$\mathbf{c}_{T3}$ and $\mathbf{C}_{T3}$HPQ$\mathbf{c}_{T3}$RGD$\mathbf{c}_{T3}$ were identified as the most potent RGD bicycle binders to integrin $\alpha_v\beta_3$.

Determination of Affinity Binding Constants (K_d). We also studied the bicycle−integrin interaction in a direct manner using surface plasmon-enhanced fluorescence spectroscopy (SPFS),[19] an optical technique that combines surface plasmon resonance (SPR) with fluorescence spectroscopy. For that purpose, (i) the bicycle-peptide $\mathbf{C}_{T3}$HPQ$\mathbf{c}_{T3}$RGD$\mathbf{c}_{T3}$ (best third-generation binder), (ii) linear GRGDS, (iii) *cyclo*-[KRGDf] and (iv) knottin-RGD were resynthesized including an N-terminal linker (K-PPPSG[Abz]SG, Abz = 4-amino-benzoic acid) following earlier studies of Pallarola et al. showing this linker to be minimally invasive with integrin affinity.[20] The N-terminal lysine was acetylated, while the lysine side-chain amine was deprotected. Since the use of conventional SPR lacked sensitivity (data not shown), probably due to the low molecular weight (~2 kDa) of the bicycles, the peptides were labeled with the fluorescent Cy5 tag via coupling of a Cy5-NHS activated ester to the lysine side-chain amine, and the surface plasmon field intensity was applied at the wavelength coincident with the absorption band of Cy5 to locally excite a fluorescence signal in close proximity to the gold surface. This approach increases the fluorescence signal originating from the peptide binding at the surface with an immobilized integrin receptor, which allows kinetic measurements.[19] Concentration-dependent fluorescence curves $F(c)$ were normalized to ΔF_{max} (value measured at saturation concentration) and fitted via Langmuir isotherm (Figure 3A). The dissociation equilibrium constant (K_d) was determined for Cy5-labeled $\mathbf{C}_{T3}$HPQ$\mathbf{c}_{T3}$RGD$\mathbf{c}_{T3}$, which turned out to be comparable to that of Cy5-labeled knottin-RGD (0.6 nM, Figure 3B). These results perfectly align with the competition ELISA data (Figure 2A). For Cy5-labeled *cyclo*-[KRGDf], a slightly weaker affinity (K_d = 4.1 nM) was determined, indicating that Cy5 labeling affects $\alpha_v\beta_3$ binding of *cyclo*-[KRGDf] more significantly than for knottin-RGD or the bicyclic peptide (see IC_{50} values, Figure 2A). The linear peptide Cy5-GRGDS did not show measurable binding to $\alpha_v\beta_3$ in SPFS.

Selectivity of Bicycle Binding to $\alpha_v\beta_3$. Finally, we compared the $\alpha_v\beta_3$ binding abilities of $\mathbf{C}_{T3}$HPQ$\mathbf{c}_{T3}$RGD$\mathbf{c}_{T3}$, $\mathbf{C}_{T3}$HPQ$\mathbf{C}_{T3}$RGD$\mathbf{c}_{T3}$, and $\mathbf{C}_{T3}$HSQ$\mathbf{C}_{T3}$RGD$\mathbf{c}_{T3}$, the three highest-affinity bicycle peptides, and control peptides (knottin-RGD and *cyclo*-[KRGDf]) with the corresponding binding values for integrins $\alpha_5\beta_1$ and $\alpha_v\beta_5$ by measuring IC_{50} values in

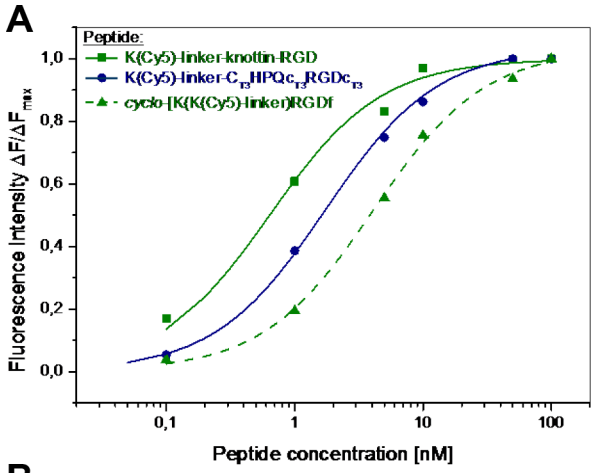

B

Peptide	K_d [nM]
K(Cy5)-linker-$\mathbf{C}_{T3}$HPQ$\mathbf{c}_{T3}$RGD$\mathbf{c}_{T3}$	0.4
K(Cy5)-linker-GRGDS	>100
cyclo-[K(K(Cy5)-linker)RGDf]	4.1
K(Cy5)-linker-knottin-RGD	0.6

Figure 3. (A) Concentration-dependent, normalized fluorescence signals for selected Cy5-labeled peptide binding to integrin $\alpha_v\beta_3$; (B) Overview of measured equilibrium dissociation constants (K_d). Linker: PPPSG[4-Abz]SG.

competition ELISA. We found that none of the three bicycle peptides showed any measurable interaction with either $\alpha_v\beta_5$ nor $\alpha_5\beta_1$ (IC_{50} > 10000 nM), which highlights their outstanding selectivities for $\alpha_v\beta_3$ (Table 1). In sharp contrast

Table 1. IC_{50} Values Determined Using Competition ELISA for Three Best-Binding RGD Bicycle Peptides, *cyclo*-[KRGDf], Cilengitide, and Knottin-RGD for Different Integrins[a]

	IC_{50} (nM)		
peptide	$\alpha_v\beta_3$	$\alpha_v\beta_5$	$\alpha_5\beta_1$
$\mathbf{C}_{T3}$HPQ$\mathbf{c}_{T3}$RGD$\mathbf{c}_{T3}$	30 ± 4	>10000	>10000
$\mathbf{C}_{T3}$HPQ$\mathbf{C}_{T3}$RGD$\mathbf{c}_{T3}$	31 ± 2	>10000	>10000
$\mathbf{C}_{T3}$HSQ$\mathbf{C}_{T3}$RGD$\mathbf{c}_{T3}$	42 ± 6	>10000	>10000
cyclo-[KRGDf]	35 ± 6	182 ± 29	>10000
cilengitide	121 ± 18	26 ± 5	>10000
knottin-RGD	38 ± 5	76 ± 7	114 ± 8

[a]Each concentration was tested in triplicate. IC_{50} values were calculated via nonlinear regression analysis using GraphPad.

to this, *cyclo*-[KRGDf] did show strong binding to $\alpha_v\beta_5$ (IC_{50} = 182 nM) while not to $\alpha_5\beta_1$, whereas knottin-RGD bound to all integrins with equally strong affinity ($\alpha_v\beta_5$, IC_{50} = 76 nM; $\alpha_5\beta_1$, IC_{50} = 114 nM). These data reveal that bicyclic RGD peptides display $\alpha_v\beta_3$ selectivities superior to benchmark RGD peptides, such as knottin-RGD, *cyclo*-[KRGDf] and cilengitide.[12] Recently, Neubauer et al. described peptidomimetics with $\alpha_v\beta_3/\alpha_5\beta_1$ selectivity ratios of ~0.006 and ~0.007 (ratio of corresponding IC_{50} values),[13f] which is still at least 2-fold less selective in comparison to the highest-affinity bicyclic $\alpha_v\beta_3$ binder $\mathbf{C}_{T3}$HPQ$\mathbf{c}_{T3}$RGD$\mathbf{c}_{T3}$, for which this ratio is ≤0.003.

DOI: 10.1021/acscombsci.8b00144
ACS Comb. Sci. 2019, 21, 198−206

Structural Analysis via 2D-NMR Spectroscopy. Bicycle peptide $\mathbf{C}_{T3}$HPQ$\mathbf{C}_{T3}$RGD$\mathbf{c}_{T3}$ was studied in detail by NMR using different techniques (COSY/ROESY/TOCSY/HSQC). Individual residues were identified through their ^{1}H and ^{13}C (in particular H_α/C_α) chemical shifts (from edited HSQC) as well as chemical shifts of the side-chain resonances (2D TOCSY). From these data it can be concluded that the peptide largely adopts a random coil structure rather than an ordered secondary structure (Figure 4). This is fully in line with data from circular dichroism spectroscopy (data not shown) that were also representative of mainly random-coil structures in solution. Another possibility is that the peptide adopts a different folded structure—apart from α-helix or β-sheet—that cannot be detected with 2D NMR techniques. Interestingly, the histidine residue shows a double set of aromatic proton resonances at 8.66/8.60 and 7.33/7.29 ppm, which according to 1D/2D-ROESY experiments are belonging to different conformers in chemical exchange. Given the slight differences in ^{1}H and ^{13}C chemical shifts of the exchanging histidines, it is unlikely the effect arises from π/τ tautomerism. Rather, a more likely explanation is that two different proline conformations coexist (~3:1 ratio), which influences the chemical shifts of neighboring residues, such as histidine and the *N*-acetyl methyl resonance (1.91/2.03 ppm). This is supported by the significant differences in the proline diastereotopic H_δ resonances (3.92 vs 3.66 ppm and 3.75 vs 3.50 ppm), and the effect diminishes as one moves farther away from the proline. Considering the sharpness of the resonances, relaxation measurements were not pursued, as the structure is most likely monomeric.

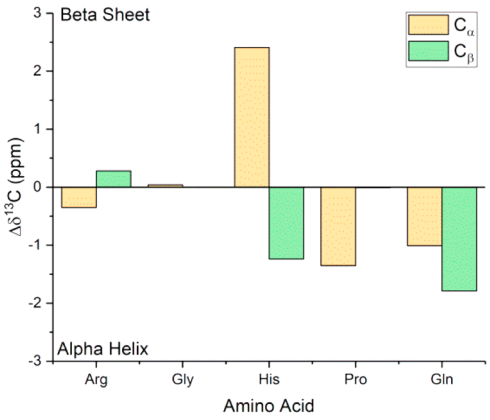

Figure 4. Chemical shift difference plots for C_α and C_β calculated by $\Delta\delta(^{13}C_\alpha) = \delta(^{13}C_{\alpha,rc}) - \delta(^{13}C_{\alpha,i})$ and $\Delta\delta(^{13}C_\beta) = \delta(^{13}C_{\beta,i}) - \delta(^{13}C_{\beta,rc})$ (i = measured amino acid in bicycle, rc = random coil chemical shift). Positive values reflect more β-sheet character, while negative values represent more α-helical character. Amino acids that are close to the baseline are indicative of a random coil structure or show both α-helical and β-sheet character or alternatively structured sequences.

Membrane Binding on Integrin-Expressing Cells (HT29). In order to prove that RGD bicycles also bind to integrins in their natural environment of the cell membrane, we labeled human colon cancer cells (HT29, express integrin α_v subunit) with the Cy5-functionalized bicycle peptide $\mathbf{C}_{T3}$HPQ$\mathbf{C}_{T3}$RGD$\mathbf{c}_{T3}$, knottin-RGD, and *cyclo*-[KRGDf] and detected fluorescence emission via confocal microscopy. Surprisingly, the bicycle shows very high staining levels, much higher than that of the Cy5-labeled benchmark knottin-RGD (Figure 5), while the Cy5-labeled *cyclo*-[KRGDf] peptide is virtually silent under these conditions. Thereby, the peptide is clearly located on the cell membrane and is hardly internalized. Control studies with scrambled RGD bicycles showed did not show any traces of cell staining (data not shown), which proves that binding is clearly sequence specific. These data illustrate the potential of RGD bicycles as powerful markers of integrin expression on live cells.

CONCLUSION

In this study, we presented bicyclic RGD "CLIPS" peptides as a novel platform for high-affinity and -selectivity integrin $\alpha_v\beta_3$ binders. These peptides offer a straightforward, cost-effective, and versatile alternative for established binders, such as knottin-RGD and cyclo-[KRGDf]. The observed high selectivity for integrin $\alpha_v\beta_3$ suggests applications in integrin-mediated in vivo tumor staining, cancer diagnostics, and/or cancer therapeutics."

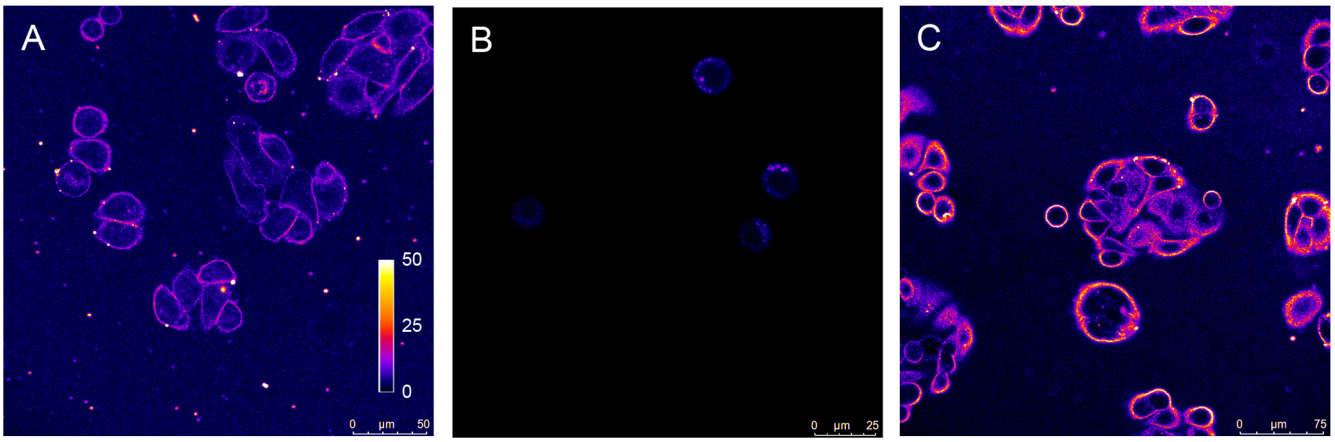

Figure 5. Confocal microscopy images of HT29 cells incubated with benchmarks Cy5-linker-knottin-RGD (A), *cyclo*-[K(Cy5-linker)RGDf] (B), and bicycle Cy5-linker-$\mathbf{C}_{T3}$HPQ$\mathbf{c}_{T3}$RGD$\mathbf{c}_{T3}$ (C). Cells were incubated on glass coverslips for at least 24 h, followed by addition of Cy5-labeled peptides for 30 min at 4 °C, washing, fixation with 4% PFA, and finally confocal analysis. All images were acquired under identical imaging conditions and processed via ImageJ (LUT: Fire). The contrast is shown in arbitrary units (au): 0, no fluorescence; 50, maximum fluorescence.

DOI: 10.1021/acscombsci.8b00144
ACS Comb. Sci. 2019, 21, 198−206

MATERIALS AND METHODS

Reagents and Chemicals. Incubation and washing buffers were prepared using standard protocols. Recombinant human integrins were purchased from R&D Systems (Minneapolis, USA). Strep-HRP (Streptavidin-Horseradish Peroxidase conjugate, Southern-Biotech, Birmingham, USA), was diluted 1:1000 for ELISA experiments. Amino acids were purchased from Iris Biotech (Marktredwitz, Germany) and Matrix Innovation (Quebec, Canada). Resins were purchased from Rapp Polymere (Tübingen, Germany) and Merck (Darmstadt, Germany). $MnCl_2 \cdot 4H_2O$, 1,3,5-tris(bromomethyl)benzene (**T3**), 1,3-bis(bromomethyl)-benzene (**mT2**), 2,2-dithiobis(5-nitropyridine) (DTNP), ethyl(dimethylaminopropyl)-carbodiimide (EDC), *N*-hydroxysuccinimide (NHS), ethanolamine, Tween20, ethylene glycol, and acetic acid and sodium acetate for the preparation of acetate buffer were purchased from Sigma-Aldrich (Steinheim, Germany). $CaCl_2 \cdot 2H_2O$, $MgCl_2 \cdot 6H_2O$, and phosphate-buffered saline (PBS) were purchased from Merck (Darmstadt, Germany). Tween80 was purchased from Faryon (Capelle, The Netherlands), and I-Block was purchased from Tropix (Bedford, USA). Disulfo-Cy5-NHS ester was purchased from Cyandye (Sunny Isles Beach, USA). Dithiolaromatic PEG6-carboxylate (thiol-COOH; SPT0014A6) and dithiolaromatic PEG3 (thiolPEG); SPT-0013) were purchased from SensoPath Technologies (Bozeman, USA). Sodium *p*-tetrafluorophenol-sulfonate (TFPS) and *S*-3-(benzoylphenoxy)propyl ethanethioate (thiol-benzophenone) were synthesized at the Max Planck Institute for Polymer Research (Mainz, Germany) according to the literature.[21,22] Poly(*N*-isopropylacrylamide)-based terpolymer with a 94:5:1 molar ratio of *N*-isopropylacrylamide, methacrylic acid, and 4-methacryloyloxy benzophenone (pNIPAAm) were synthesized as previously described.[23,24]

Peptide Synthesis. Synthesis of crude bicyclic peptide libraries, purified bicyclic and monocyclic peptides, and Cy5-labeled peptides was performed using standard Fmoc-based peptide synthesis. All 672 peptides were synthesized and collected separately (synthesis on 2 μmol scale on solid phase, collection in 96-well polypropylene storage plates (each 2 mL). For more detailed information, see the Supporting Information

ELISA. For buffer compositions and concentrations, see Table S-1 in the Supporting Information.

Integrin Coating and Blocking. Plates were coated with 100 μL of a 0.25−0.5 μg/mL integrin solution in coating buffer onto 96-well NUNC Polysorp plates (overnight, 4 °C) followed by blocking with 150 μL of 1% I-Block in blocking buffer (60 min, room temperature) and 3× washing with 400 μL of washing buffer.

Library Screening. In each screening experiment, 96 or 192 different peptides were tested. Bicyclic peptide libraries (2 μmol) were dissolved in DMSO (10 mM stock solutions) and further diluted to working concentrations (1 mM to 2.5 μM) with incubation buffer. After incubation with a fixed concentration of biotinylated knottin-RGD peptide in incubation buffer (minimum 15 min, room temperature), the individual bicycle solutions were added to the integrin-coated plates (90 min, room temperature), followed by 3× washing with washing buffer. Then the plates were incubated with 100 μL of 1:1000 Strep-HRP in Strep-HRP buffer (60 min, room temperature). After 4× washing they were incubated with 150 μL of substrate buffer containing 0.91 mM ABTS (2,2′-azino-bis(3-ethylbenzothiazoline-6-sulfonic acid) and 0.006% H_2O_2 in substrate buffer (0.2 M Na_2HPO_4 adjusted to pH 4 using 0.2 M citric acid). Absorbance (405 nm) was measured after 4 min using a Molecular Devices Spectramax M2 plate reader.

IC_{50} Determination. Peptides were mixed in eight different concentrations (each 3-fold dilutions) with a fixed concentration of biotinylated knottin-RGD (both in incubation buffer, 15 min, room temperature), followed by incubation of the plates with peptide/biotinylated knottin-RGD solutions for 90 min at room temperature. Strep-HRP and ABTS incubation steps were performed as described for library screening. All concentrations were tested in triplicate. IC_{50} values were calculated via nonlinear regression analysis using GraphPad Prism software and represent the peptide concentration at which 50% inhibition of biotinylated knottin binding is observed.

Surface Plasmon-Enhanced Fluorescence Spectroscopy (SPFS). For the description of the optical system, sensor chip preparation, and the immobilization of the ligand, see the Supporting Information.

Measurement of Equilibrium Dissociation Constant K_d. For measurement of the binding affinity of Cy5-labeled peptides to immobilized integrin ligands, PBS with 1 mM $CaCl_2$, 0.5 mM $MnCl_2$, 1 mg/mL BSA, and 0.05% Tween20 was used as the running buffer. Different concentrations of the peptide (0.1, 1, 5, 10, 50, 100, and 1000 nM) were sequentially flushed over the sensor surface. The sample at each concentration was allowed to react with the integrin for 30 min followed by rinsing the surface with running buffer solution for 10 min. The binding of the target analyte was monitored in real time by measuring the fluorescence intensity $F(t)$ originating from the close proximity to the sensor surface that was probed by resonantly excited surface plasmons (Figure S-4B in the Supporting Information). The fluorescence signal F gradually increased upon binding of target analyte, and for each concentration, the equilibrium fluorescence signal ΔF was determined as a difference to the fluorescence baseline after 10 min of rinsing with running buffer. The titration curve was established on the basis of these values, and it was fitted with a Langmuir isotherm model (function $\Delta F = \Delta F_{max} c/(K_d + c)$) in order to determine the equilibrium dissociation constant K_d.

NMR. A detailed description of the acquisition of the NMR spectra, devices, methods, and spectrum editing, as well as the ^{1}H NMR spectrum of the bicycle $\mathbf{C}_{T3}$HPQ$\mathbf{c}_{T3}$RGD$\mathbf{c}_{T3}$ (Figure S-5) is depicted in the Supporting Information. T_1 measurements were performed by properly calibrating the 90° pulse length and then performing estimates using the 1D inversion recovery sequence with excitation sculpting water suppression. After the longest T_1 was determined to be approximately 2 s, a pseudo-2D inversion recovery experiment was performed with 10 separate delays of 8 scans each with a total longitudinal relaxation time of 10.3 s. T_2 measurements were acquired by first performing estimates using the 1D PROJECT-CMPG sequence[25] with presaturation water suppression. After the longest T_2 was determined to be approximately 1 s, a pseudo-2D PROJECT-CPMG sequence experiment with presaturation was performed with 12 separate delays of 8 scans each and a cycle time of 4 ms with a total longitudinal relaxation time of 10.3 s.

Cell Integrin Staining and Confocal Microscopy. Human colorectal adenocarcinoma cells (HT29) were obtained from The Netherlands Cancer Institute (NKI) and grown using standard procedures and conditions. For the

DOI: 10.1021/acscombsci.8b00144
ACS Comb. Sci. 2019, 21, 198−206

experiment, the cells were allowed to adhere on clean glass coverslips for at least 24 h until they reached approximately 40−50% confluency. Then, the glass coverslips were washed two times with cold HCG buffer (carbonate-buffered saline, pH 7.2, containing 140 mM NaCl, 5 mM KCl, 23 mM $NaHCO_3$, 10 mM HEPES, 10 mM glucose, 1 mM $CaCl_2$, 0.5 mM $MgCl_2$, and 0.5 mM $MnCl_2$) to remove nonadhered cells, followed by adding cold HCG buffer and cooling of the glass coverslips to 4 °C. Afterward, the Cy5-labeled peptides were added and allowed to incubate at 1 μM for 30 min at 4 °C, followed by at least five washing steps with HCG buffer, fixation with 4% paraformaldehyde solution in PBS pH 7.4 (20 min), and another four washing steps with HCG buffer. Subsequently, the cells were analyzed via confocal microscopy using a Leica TCS SP8 confocal microscope equipped with a supercontinuum white light laser (NKT Photonics) and water immersion objectives (63x W PL APO CS2, NA 1.2/40x W PL APO CS2, NA 1.1). The excitation wavelength was set to 633 nm while fluorescence was detected from 646 to 778 nm. All images were acquired under identical imaging conditions and processed via ImageJ (LUT: Fire).

■ ASSOCIATED CONTENT

Supporting Information

The Supporting Information is available free of charge on the ACS Publications website at DOI: 10.1021/acscombsci.8b00144.

Structures of (biotinylated) knottin-RGD and *cyclo*-[KRGDf], detailed information about peptide synthesis, analysis, and purification and amino acids used in peptide libraries, additional peptides screened, and structure of biotinylated knottin-RGD peptide, parameters varied in the competition ELISA setup, inhibition values for selected bicyclic peptides and monocyclic analogues, position-replacement analysis for cysteines, ELISA protocol for testing HPQ-streptavidin binding and results, description and schematic of optical instrument used for SPFS and ligand immobilization, SPR sensorgrams and SPFS measurement for Cy5-functionalized bicycle $\mathbf{C_{T3}}$HPQ$\mathbf{c_{T3}}$RGD$\mathbf{c_{T3}}$, additional NMR information, and ^{1}H NMR spectrum of bicycle $\mathbf{C_{T3}}$HPQ$\mathbf{c_{T3}}$RGD$\mathbf{c_{T3}}$ (PDF)

■ AUTHOR INFORMATION

Corresponding Author

*P.T.: tel, +31-320-225300; fax, +31-320-225301; e-mail, p.timmerman@pepscan.com.

ORCID

Jakub Dostalek: 0000-0002-0431-2170

Peter Timmerman: 0000-0001-6687-5297

Author Contributions

The manuscript was written through contributions of all authors. D.B. and P.T. conceived the concept and analyzed the data. D.B. performed peptide syntheses, competition and binding ELISA experiments, and in vitro integrin staining experiments. V.J., N.G.Q., and J.D. designed, performed, and analyzed the SPR experiments. P.B.W. performed and analyzed the NMR experiments. D.B., K.J. and P.T. evaluated the confocal images. D.B., P.B.W., and P.T. wrote the manuscript. All authors have given approval to the final version of the manuscript.

Notes

The authors declare the following competing financial interest(s): Pepscan is the inventor of the CLIPS technology and holds a patent on the synthesis of bicyclic peptides using 2-CLIPS technology.

■ ACKNOWLEDGMENTS

This project received funding from Horizon-2020 research and innovation program BIOGEL under the Marie Sklodowska-Curie grant agreement No. 64268.

■ REFERENCES

(1) (a) Driggers, E. M.; Hale, S. P.; Lee, J.; Terrett, N. K. The exploration of macrocycles for drug discovery — an underexploited structural class. *Nat. Rev. Drug Discovery* **2008**, *7*, 608−624. (b) Craik, D. J.; Fairlie, D. P.; Liras, S.; Price, D. The Future of Peptide-based Drugs. *Chem. Biol. Drug Des.* **2013**, *81*, 136−147. (c) Wang, C. K.; Craik, D. J. Cyclic peptide oral bioavailability: Lessons from the past. *Biopolymers* **2016**, *106*, 901−909.

(2) Timmerman, P.; Beld, J.; Puijk, W. C.; Meloen, R. H. Rapid and quantitative cyclization of multiple peptide loops onto synthetic scaffolds for structural mimicry of protein surfaces. *ChemBioChem* **2005**, *6*, 821−824.

(3) (a) Li, P.; Roller, P. P. Cyclization strategies in peptide derived drug design. *Curr. Top. Med. Chem.* **2002**, *2*, 325−341. (b) Baeriswyl, V.; Heinis, C. Polycyclic Peptide Therapeutics. *ChemMedChem* **2013**, *8*, 377−384.

(4) Heinis, C.; Rutherford, T.; Freund, S.; Winter, G. Phage-encoded combinatorial chemical libraries based on bicyclic peptides. *Nat. Chem. Biol.* **2009**, *5*, 502−507.

(5) Angelini, A.; Cendron, L.; Chen, S.; Touati, J.; Winter, G.; Zanotti, G.; Heinis, C. Bicyclic peptide inhibitor reveals large contact interface with a protease target. *ACS Chem. Biol.* **2012**, *7*, 817−821.

(6) Rentero Rebollo, I.; McCallin, S.; Bertoldo, D.; Entenza, J. M.; Moreillon, P.; Heinis, C. Development of Potent and Selective S. aureus Sortase A Inhibitors Based on Peptide Macrocycles. *ACS Med. Chem. Lett.* **2016**, *7*, 606−611.

(7) Luzi, S.; Kondo, Y.; Bernard, E.; Stadler, L. K. J.; Vaysburd, M.; Winter, G.; Holliger, P. Subunit disassembly and inhibition of TNFα by a semi-synthetic bicyclic peptide. *Protein Eng., Des. Sel.* **2015**, *28*, 45−52.

(8) Lian, W.; Jiang, B.; Qian, Z.; Pei, D. Cell-permeable bicyclic peptide inhibitors against intracellular proteins. *J. Am. Chem. Soc.* **2014**, *136*, 9830−9833.

(9) Trinh, T. B.; Upadhyaya, P.; Qian, Z.; Pei, D. Discovery of a Direct Ras Inhibitor by Screening a Combinatorial Library of Cell-Permeable Bicyclic Peptides. *ACS Comb. Sci.* **2016**, *18*, 75−85.

(10) Timmerman, P.; Barderas, R.; Desmet, J.; Shochat, S.; Monasterio, A.; Casal, J. I.; Meloen, R. H. A combinatorial approach for the design of complementarity-determining region-derived peptidomimetics with in vitro anti-tumoral activity. *J. Biol. Chem.* **2009**, *284*, 34126−34134.

(11) (a) Barczyk, M.; Carracedo, S.; Gullberg, D. Integrins. *Cell Tissue Res.* **2010**, *339*, 269−280. (b) Takada, Y.; Ye, X.; Simon, S. The Integrins. *Genome Biol.* **2007**, *8*, 215.

(12) Dechantsreiter, M. A.; Planker, E.; Matha, B.; Lohof, E.; Jonczyk, A.; Goodman, S. L.; Kessler, H. *N*-Methylated Cyclic RGD Peptides as Highly Active and selective $\alpha_V\beta_3$ integrin antagonists. *J. Med. Chem.* **1999**, *42*, 3033−3040.

(13) (a) Marinelli, L.; Lavecchia, A.; Gottschalk, K.-E.; Novellino, E.; Kessler, H. for example, see:_Docking studies on alphavbeta3 integrin ligands: pharmacophore refinement and implications for drug design. *J. Med. Chem.* **2003**, *46*, 4393−4404. (b) Heckmann, D.; Meyer, A.; Marinelli, L.; Zahn, G.; Stragies, R.; Kessler, H. Probing integrin selectivity: rational design of highly active and selective ligands for the $\alpha_5\beta_1$ and $\alpha_v\beta_3$ integrin receptor. *Angew. Chem., Int. Ed.* **2007**, *46*, 3571−3574. (c) Bochen, A.; Marelli, U. K.; Otto, E.; Pallarola, D.; Mas-Moruno, C.; Saverio, F.; Leva, D.; Boehm, H.;

DOI: 10.1021/acscombsci.8b00144
ACS Comb. Sci. 2019, 21, 198−206

Spatz, J. P.; Novellino, E.; Kessler, H.; Marinelli, L. Biselectivity of iso DGR Peptides for Fibronectin Binding Integrin Subtypes $\alpha_5\beta_1$ and $\alpha_v\beta_6$: Conformational Control through Flanking Amino Acids. *J. Med. Chem.* **2013**, *56*, 1509−1519. (d) Rechenmacher, F.; Neubauer, S.; Polleux, J.; Mas-Moruno, C.; De Simone, M.; Cavalcanti-Adam, E. A.; Spatz, J. P.; Fässler, R.; Kessler, H. Functionalizing $\alpha_v\beta_3$- or $\alpha_5\beta_1$-selective integrin antagonists for surface coating: A method to discriminate integrin subtypes in vitro. *Angew. Chem., Int. Ed.* **2013**, *52*, 1572−1575. (e) Hegemann, J. D.; De Simone, M.; Zimmermann, M.; Knappe, T. A.; Xie, X.; Di Leva, F. S.; Marinelli, L.; Novellino, E.; Zahler, S.; Kessler, H.; Marahiel, M. A. Rational improvement of the affinity and selectivity of integrin binding of grafted lasso peptides. *J. Med. Chem.* **2014**, *57*, 5829−5834. (f) Neubauer, S.; Rechenmacher, F.; Brimioulle, R.; Saverio, F.; Leva, D.; Bochen, A.; Sobahi, T. R.; Schottelius, M.; Novellino, E.; Mas-Moruno, C.; Marinelli, L.; Kessler, H. Pharmacophoric Modifications Lead to Superpotent $\alpha_v\beta_3$ Integrin Ligands with Suppressed $\alpha_5\beta_1$ Activity. *J. Med. Chem.* **2014**, *57*, 3410−3417. (g) Maltsev, O. V.; Marelli, U. K.; Kapp, T. G.; Di Leva, F. S.; Di Maro, S.; Nieberler, M.; Reuning, U.; Schwaiger, M.; Novellino, E.; Marinelli, L.; Kessler, H. Stable Peptides Instead of Stapled Peptides: Highly Potent $\alpha_v\beta_6$-Selective Integrin Ligands. *Angew. Chem., Int. Ed.* **2016**, *55*, 1535−1539. (h) Kruss, S.; Wolfram, T.; Martin, R.; Neubauer, S.; Kessler, H.; Spatz, J. P. Stimulation of Cell Adhesion at Nanostructured Teflon Interfaces. *Adv. Mater.* **2010**, *22*, 5499−5506. (i) Kruss, S.; Erpenbeck, L.; Amschler, K.; Mundinger, T. A.; Boehm, H.; Helms, H.-J.; Friede, T.; Andrews, R. K.; Schön, M. P.; Spatz, J. P. Adhesion Maturation of Neutrophils on Nanoscopically Presented Platelet Glycoprotein Ibα. *ACS Nano* **2013**, *7*, 9984−9996. (j) Polo, E.; Nitka, T. T.; Neubert, E.; Erpenbeck, L.; Vukovic, L.; Kruss, S. Control of integrin affinity by confining peptides on fluorescent carbon nanotubes. *ACS Appl. Mater. Interfaces* **2018**, *10*, 17693−17703.

(14) (a) Kimura, R. H.; Levin, A. M.; Cochran, F. V.; Cochran, J. R. Engineered cystine knot peptides that bind $\alpha_v\beta_3$, $\alpha_v\beta_5$, and $\alpha_5\beta_1$ integrins with low-nanomolar affinity. *Proteins: Struct., Funct., Genet.* **2009**, *77*, 359−369. (b) Kimura, R. H.; Teed, R.; Hackel, B. J.; Pysz, M. A.; Chuang, C. Z.; Sathirachinda, A.; Willmann, J. K.; Gambhir, S. S. Pharmacokinetically Stabilized Cystine Knot Peptides that bind Alpha-v-Beta-6 Integrin with Single-Digit Nanomolar Affinities for Detection of Pancreatic Cancer. *Clin. Cancer Res.* **2012**, *18*, 839−849. (c) Kim, J. W.; Cochran, F. V.; Cochran, J. R. A Chemically Cross-Linked Knottin Dimer Binds Integrins with Picomolar Affinity and Inhibits Tumor Cell Migration and Proliferation. *J. Am. Chem. Soc.* **2015**, *137*, 6−9.

(15) Timmerman, P.; Beld, J.; Meloen, R. H.; Puijk, W. C. Method for Selecting a Candidate Drug Compound. WO/2004/077062, 2004.

(16) Bernhagen, D.; De Laporte, L.; Timmerman, P. High-Affinity RGD-Knottin Peptide as a New Tool for Rapid Evaluation of the Binding Strength of Unlabeled RGD-Peptides to $\alpha_v\beta_3$, $\alpha_v\beta_5$, and $\alpha_5\beta_1$ Integrin Receptors. *Anal. Chem.* **2017**, *89*, 5991−5997.

(17) Aumailley, M.; Gurrath, M.; Calvete, J.; Timpl, R.; Kessler, H. Arg-Gly-Asp constrained within cyclic pentapeptides - Strong and selective inhibitors of cell adhesion to vitronectin and laminin fragment P1. *FEBS Lett.* **1991**, *291*, 50−54.

(18) Giebel, L. B.; Cass, R. T.; Milligan, D. L.; Young, D. C.; Arze, R.; Johnson, C. R. Screening of cyclic peptide phage libraries identifies ligands that bind streptavidin with high affinities. *Biochemistry* **1995**, *34*, 15430−15435.

(19) Bauch, M.; Toma, K.; Toma, M.; Zhang, Q.; Dostalek, J. Surface plasmon-enhanced fluorescence biosensors: a review. *Plasmonics* **2014**, *9*, 781−799.

(20) Pallarola, D.; Bochen, A.; Boehm, H.; Rechenmacher, F.; Sobahi, T. R.; Spatz, J. P.; Kessler, H. Interface immobilization chemistry of cRGD-based peptides regulates integrin mediated cell adhesion. *Adv. Funct. Mater.* **2014**, *24*, 943−956.

(21) Beines, P. W.; Klosterkamp, I.; Menges, B.; Jonas, U.; Knoll, W. Responsive Thin Hydrogel Layers from Photo-Cross-Linkable Poly(*N*-isopropylacrylamide) Terpolymers. *Langmuir* **2007**, *23*, 2231−2238.

(22) Gee, K. R.; Archer, E. A.; Kang, H. C. 4-Sulfotetrafluorophenyl (STP) esters: New water-soluble amine-reactive reagents for labeling biomolecules. *Tetrahedron Lett.* **1999**, *40*, 1471−1474.

(23) Junk, M. J. N.; Jonas, U.; Hinderberger, D. EPR spectroscopy reveals nanoinhomogeneities in the structure and reactivity of thermoresponsive hydrogels. *Small* **2008**, *4*, 1485−1493.

(24) Anac, I.; Aulasevich, A.; Junk, M. J. N.; Jakubowicz, P.; Roskamp, R. F.; Menges, B.; Jonas, U.; Knoll, W. Optical Characterization of Co-Nonsolvency Effects in Thin Responsive PNIPAAm-Based Gel Layers Exposed to Ethanol/Water Mixtures. *Macromol. Chem. Phys.* **2010**, *211*, 1018−1025.

(25) Aguilar, J. A.; Nilsson, M.; Bodenhausen, G.; Morris, G. A. Spin echo NMR spectra without J modulation. *Chem. Commun.* **2012**, *48*, 811−813.

DOI: 10.1021/acscombsci.8b00144
ACS Comb. Sci. 2019, 21, 198−206